

# Heterochiral tetrapeptide self-assembly into hydrogel biomaterials for hydrolase mimicry

Marina Kurbasic | Ana M. Garcia | Simone Viada | Silvia Marchesan 

Self-assembling short peptides have attracted great interest as enzyme mimics, especially if the catalytic activity resides solely in the supramolecular structure so that it can be switched on/off as needed by controlling assembly/disassembly. Among the various enzyme classes, hydrolases find wide application in biomaterials, and their mimetics often contain His residues, in addition to either divalent cations or other amino acids to mimic the catalytic site. This work reports two self-assembling tetrapeptides based on the Ser-His motif for catalysis and the Phe-Phe motif to drive amyloid structure formation. Both peptides form thermoreversible hydrogels in phosphate buffer at neutral pH that display a mild esterase-like activity, as demonstrated on the hydrolysis of 4-nitrophenyl acetate as a model substrate, although presence of Ser did not enhance catalytic activity. The systems are characterised by circular dichroism, transmission electron microscopy, oscillatory rheology and Thioflavin T fluorescence as an amyloid stain, to provide further insights that may assist the future design of improved supramolecular catalysts.

## KEYWORDS

amyloid, biocatalysis, biomaterials, enzyme mimicry, esterase, hydrogels, phenylalanine, Phe-Phe

## 1 | INTRODUCTION

Enzymes have long inspired scientists for their exquisite ability to catalyse chemical reactions with great selectivity and at mild conditions. Among the various enzymatic classes, hydrolases represent a good target for mimicry as they are widely used by the industry and, generally, in organic synthesis. They include proteases and lipases, which are among the most popular choice in synthetic strategies. They have been widely employed for the green synthesis of biomaterials and biopolymers,<sup>1</sup> and the latter have been widely used to anchor enzymes for enhanced activity and stability.<sup>2</sup> The link between hydrolases and biomaterials has been strong for years. For instance, metalloproteinases are well-known for their active roles in tissue repair and remodelling<sup>3</sup> and have long been studied for the development of biomaterials. Often, biomaterials contain hydrolase-sensitive bioactive molecules that will thus be released upon enzymatic cleavage to allow the biomaterials to adapt to the microenvironment around cells.<sup>4</sup> Lipases are also heavily studied in relation to the

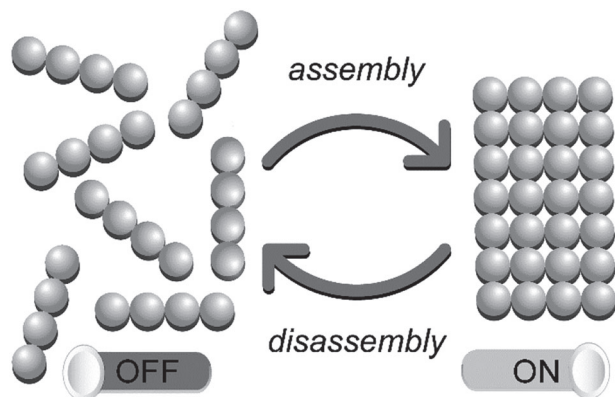
gastrointestinal absorption of lipophilic drugs for the development of innovative vehicles for their delivery.<sup>5</sup> More recently, nanostructures that are able to mimic enzymes (nanozymes) have stimulated research for their application in innovative, active biomaterials for use in theranostics and, more generally, in the biomedical field.<sup>6</sup>

Enzymes typically comprise over one hundred amino acids in their sequence, and their activity relies on correct folding that may be compromised by changes in temperature, solvent or pH. Although there is an ever increasing number of cheap enzymes that are commercially available, generally speaking, it would be more convenient to use simpler and more robust chemical structures. However, the design of enzyme mimics based on short peptides is notoriously challenging, and conformational effects must be considered carefully.<sup>7</sup> One promising class of enzyme mimetics comprises self-assembling short peptides,<sup>8</sup> which allow to include the very same functional groups present in enzymes, and with them share many advantages, such as biodegradability, and catalytic activity in water.<sup>9</sup> The self-organisation may create hydrophobic pockets that could mimic those of enzymes,

whereby hydrophobic reagents could concentrate for reactions to occur. Additionally, if activity resided solely in the assemblies, it could be switched on/off with assembly/disassembly (Scheme 1). Furthermore, the multivalency that arises from the presence of adjacent peptides in the supramolecular assemblies ensures scope for the investigation of these systems. This exciting topic has been gathering wide interest in recent years.<sup>10</sup>

A hydrolase common feature is the presence of the His residue at the catalytic site, but this typically requires further activation either by a divalent metal ion or by the functionalities of flanking amino acids. In a pioneering work, Chen et al. showed that, interestingly, His on its own does not display hydrolytic catalysis of biomolecules nor does in the dipeptide His-Ser; by contrast, notable catalytic activity was observed by using the dipeptide sequence Ser-His.<sup>11</sup> This dipeptide was reported to catalyse also the condensation of amino acids in di-, tri- or tetra-peptides, as well as the formation of peptide nucleic acids.<sup>12</sup> It is not surprising that both Ser and His have been included in the design of various peptides to identify novel catalysts.<sup>13</sup> Despite the significant amount of literature on the topic, it is yet not possible to design de novo a catalytic and self-assembling sequence based on just a few amino acids. This is exemplified by a large study by Tuttle and Ulijn whereby they scored for hydrophobicity all 8,000 L-tripeptides and among the selected sequences for self-assembly, only four new hydrogelators were described.<sup>14</sup> Further studies by Hauser et al. on unprotected tripeptide libraries also highlighted the difficulties in finding general rules of assembly.<sup>15</sup>

Nevertheless, a promising approach includes the use of the diphenylalanine motif,<sup>16</sup> and in this manner, it was possible to obtain the biocatalyst L-His-D-Phe-D-Phe (or its enantiomer D-His-L-Phe-L-Phe).<sup>17</sup> Interestingly, the biocatalytic activity towards ester hydrolysis was noted only in the assembled nanostructures, thus providing a convenient example of a supramolecular catalyst that could be switched on/off with assembly/disassembly, which could ultimately turn useful for the generation of synthetic reaction cascades. The design was based on heterochirality, as the inclusion of both D- and L-amino acids at specific positions allows to obtain self-assembly thanks to the



**SCHEME 1** A self-assembling tetrapeptide undergoes cycles of assembly/disassembly that can act as a switch for a certain (bio) activity

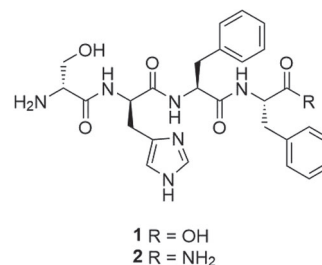
formation of amphipathic structures, whereby hydrophilic and hydrophobic components are segregated.<sup>18</sup> This approach proved useful also in the case of unprotected dipeptides.<sup>19</sup> Additional potential advantages include higher bioactivity relative to homochiral analogues for protein mimicry.<sup>20</sup> Further, presence of D-amino acids is well known to affect conformation, hence bioactivity, although not always in a predictable way.<sup>21</sup> Recently, using this strategy, also the self-assembling sequence L-His-L-Leu-D-Leu-L-Ile-L-His-L-Leu-D-Leu-L-Ile was reported to gel, but despite the presence of two His residues, the catalytic performance was only slightly better than L-His-D-Phe-D-Phe under analogous conditions.<sup>22</sup>

In light of these observations, this study aims at evaluating the self-assembling and catalytic activity of two heterochiral tetrapeptides bearing the catalytic motif Ser-His (Scheme 2), that is, D-Ser-D-His-L-Phe-L-Phe and D-Ser-D-His-L-Phe-L-Phe-NH<sub>2</sub> (amidated at the C-terminus). This choice for amino acid chirality was dictated by the need to have both Ser and His with the same stereoconfiguration as was shown to be beneficial in previous studies for the catalytic performance.<sup>11</sup> The stereoconfiguration of His was kept opposite to the Phe-Phe motif, as was the case of the previously reported supramolecular catalyst, to allow a meaningful comparison and truly assess the influence of the additional Ser residue on biocatalysis.<sup>17</sup> In addition, it should be noted that enantiomers (e.g., D-His-L-Phe-L-Phe and L-His-D-Phe-D-Phe) will display analogous supramolecular behaviour in an achiral environment. C-terminal amidation was previously noted for its positive influence on the kinetics of peptide assembly<sup>23</sup>; however, presence of the C-terminal carboxylic acid may be beneficial for the catalyst performance.<sup>12</sup> Therefore, insights into the supramolecular and catalytic behaviour of these peptides may provide valuable information for the future design of improved *smart* catalysts.

## 2 | MATERIALS AND METHODS

### 2.1 | Peptide synthesis, purification and characterisation

Peptides were synthesised and purified as described previously.<sup>24</sup> In the case of peptide **2**, a Rink amide linker was used to provide the amidated product.<sup>25</sup> Purification was performed on a reverse-phase



**SCHEME 2** The two heterochiral tetrapeptides analysed in this work; that is, D-Ser-D-His-L-Phe-L-Phe (**1**) and D-Ser-D-His-L-Phe-L-Phe-NH<sub>2</sub> (**2**)

HPLC (Agilent 1260 Infinity) using a C-18 column (Phenomenex Kinetex, 5 microns, 100 Å, 250 × 10 mm), with a gradient of acetonitrile (MeCN)/water with 0.05% TFA with the following programme:  $t = 0\text{--}2$  min. 25% MeCN;  $t = 14\text{--}16$  min. 95% MeCN ( $t_R = 7.4$  min (1) and 7.7 min (2), 98% purity). Fractions were freeze-dried to yield a fluffy and white powder (85% yield).  $^1\text{H}$  and  $^{13}\text{C}$  NMR spectra were acquired on a Varian Inova (further details can be found in the Supplementary Information).

## 2.2 | Hydrogel formation and rheology

Peptides (25 mM) were dissolved at alkaline pH (sodium phosphate 0.1 M at pH 11.5), with the aid of a short sonication and heating, by immersing the vial in a hot bath at 100°C. Upon cooling down to room temperature, hydrogels were obtained at a pH of  $7.1 \pm 0.1$ . Oscillatory rheology measurements were performed on a Kinexus Ultra Plus rheometer, with parallel-steel geometry (20-mm flat plates) at 1 Hz and 1 Pa, with the gel being formed in situ. Time sweeps were recorded for 1 h, followed by a frequency sweep at 1 Pa, and then a stress sweep at 1 Hz until gel breaking.

## 2.3 | Peptides in solution (1 mM)

Peptides (2 mM) were dissolved at alkaline pH (sodium phosphate 0.1 M at pH 11.5). Upon addition of an equal volume of mildly acidic phosphate buffer (sodium phosphate 0.1 M at pH 5.7), a 1-mM peptide solution was obtained at a pH of  $7.1 \pm 0.1$ .

## 2.4 | Circular dichroism

Circular dichroism (CD) samples were prepared as described above in 0.1-mm quartz cells on a Jasco J-815 with steps of 1 nm, resolution of 1 nm, scanning speed of 50 nm/min, 25°C unless otherwise stated. Spectra shown are the average of at least five measurements. Heating ramps were performed by acquiring the spectra every 5°C from 25°C to 75°C, then the CD signal at 228 nm was normalised and plotted against temperature (see ESI).

## 2.5 | Multiwell plate assays

Fluorescence assays using Thioflavin T (Sigma) were performed on multi-well plates in a Tecan M1000 Pro as described previously.<sup>17</sup> Briefly, 0.12 ml of gel was freshly prepared as described above and immediately placed into the wells of Greiner 96 U Bottom Transparent Polystyrene. After 4 h, 30  $\mu\text{l}$  of Thioflavin T (22  $\mu\text{M}$  in 20-mM glycine-NaOH pH 7.5, 0.2  $\mu\text{m}$  filtered) were added onto the wells. After 15 min, fluorescence was read (ex. 446 nm, em. 490 nm, 20 nm bandwidth,  $n = 6$ ). For catalysis,<sup>17</sup> each well of a 96-well plate (clear, flat bottom) was added 90  $\mu\text{l}$  of peptide at the desired concentrations

as indicated in the main text and 10  $\mu\text{l}$  of pNPA in MeOH at various concentrations as indicated in the main text. Absorbance at 405 nm was monitored over time, and each condition was repeated twice in triplicate. Average and standard deviations were calculated and plotted with Excel.

## 2.6 | TEM analysis

Transmission electron microscopy (TEM) micrographs were acquired on a Philips EM 208 equipped with Quemesa (Olympus Soft Imaging Solutions) camera; images were acquired with RADIUS software; samples were prepared as follows. Carbon-copper grids were first exposed to the UV-ozone cleaner (Procleaner Plus) for 15 min to make the grid surface more hydrophilic, then gels were precisely deposited on a TEM grid, dried for 15 min at RT, and contrasted by aqueous tungsten phosphate solution (pH 7.4).

## 3 | RESULTS AND DISCUSSION

The two tetrapeptides **1** and **2** were synthesised in solid phase according to standard protocols.<sup>24</sup> Each peptide purity was confirmed by  $^1\text{H}$  and  $^{13}\text{C}$  NMR and ESI-MS spectra (see Supporting Information). Peptide conformation in solution (1 mM) was assessed by CD spectroscopy (Figure 1A), which is a very useful technique to probe for peptide self-organisation.<sup>26</sup> Interestingly, the spectrum of **1** displayed very weak intensity, with two positive maxima at 198 and 226 nm and a negative minimum at 209 nm. By contrast, the CD spectrum of **2** was reminiscent of those of other self-assembling, heterochiral short peptides,<sup>19</sup> with two positive maxima at 199 and 219 nm, which were previously ascribed to a population of conformations in solution, of which the most stable populated the Ramachandran area of  $\beta$ -structures, including sheets and turns.<sup>27</sup>

When the concentration was increased to 25 mM, self-supporting hydrogels were obtained for both **1** and **2**. The CD spectrum of **1** could be registered only above 220 nm, and it revealed a 2-nm red-shift of the positive maximum to 228 nm, as well as presence of the vibronic signature for the aromatic residues in the 255- to 275-nm range (Figure 1B), as previously reported for the hydrogel formed by L-His-D-Phe-D-Phe.<sup>17</sup> CD heating ramps revealed a  $T_m = 50^\circ\text{C}$ , with a very sharp gel-to-sol transition (see Supplementary Information). In the case of **2**, it was not possible to register the CD spectrum in the opaque hydrogel due to excessively high-voltage during acquisition. The gel-to-sol transition was also assessed macroscopically using a hot-bath, and it was confirmed to occur at 43–61°C for **1** and 36–58°C for **2**. In both cases, the hydrogels were thermoreversible and rapidly reformed upon cooling to room temperature (Figure 1C,D).

The hydrogel nature of both compounds was confirmed by oscillatory rheology (Figure 2). Frequency sweeps confirmed both elastic ( $G'$ ) and stress ( $G''$ ) moduli were independent from the applied frequency, with  $G' > G''$  as expected for stable hydrogels (see Supporting

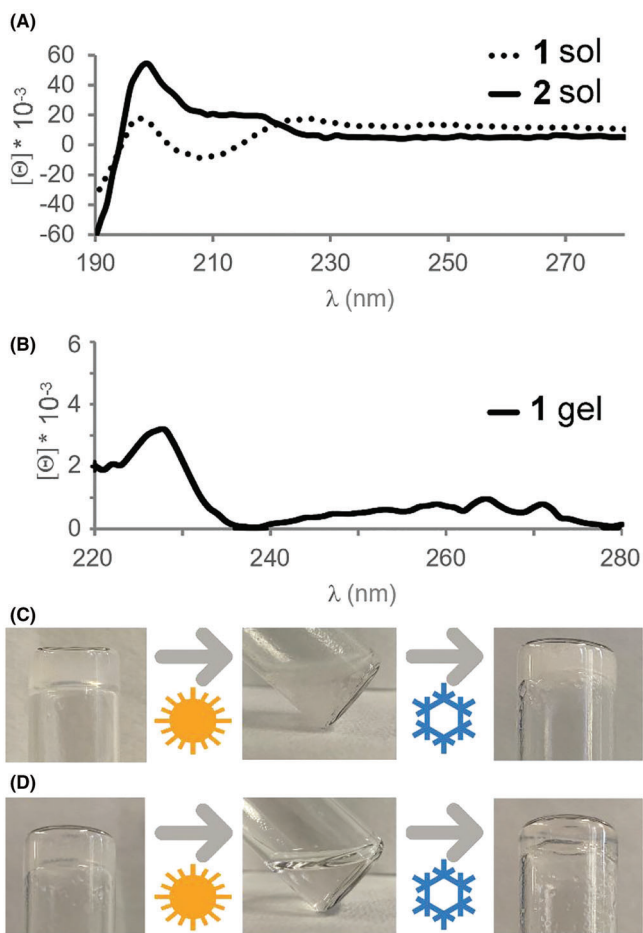


**FIGURE 1** (A) Circular dichroism (CD) spectrum of tetrapeptides in solution (1 mM). (B) CD spectrum of **1** hydrogel (25 mM). (C and D) thermoreversible nature of hydrogels from (C) **1** and (D) **2**

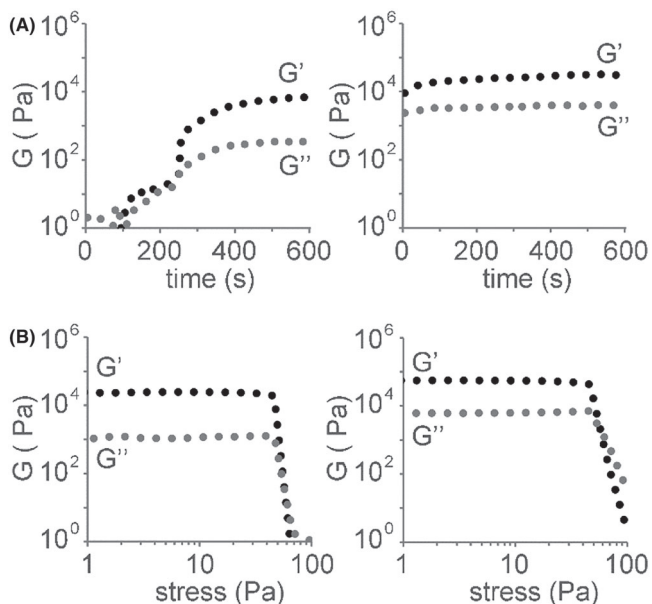


**FIGURE 2** Oscillatory rheology. (A) time sweeps for **1** (left) and **2** (right). (B) stress sweeps for **1** (left) and **2** (right)

Information). Gelation kinetics were faster for **2** relative to **1** (Figure 2A), suggesting a positive effect of C-terminal amidation, in agreement with the literature.<sup>23</sup> After an hour of assembly, **1** had reached a  $G'$  of 24 kPa against 56 kPa for **2**; both compounds displayed a linear viscoelastic region up to 50 Pa, with a rapid gel-to-sol transition occurring at higher stresses (Figure 2B).

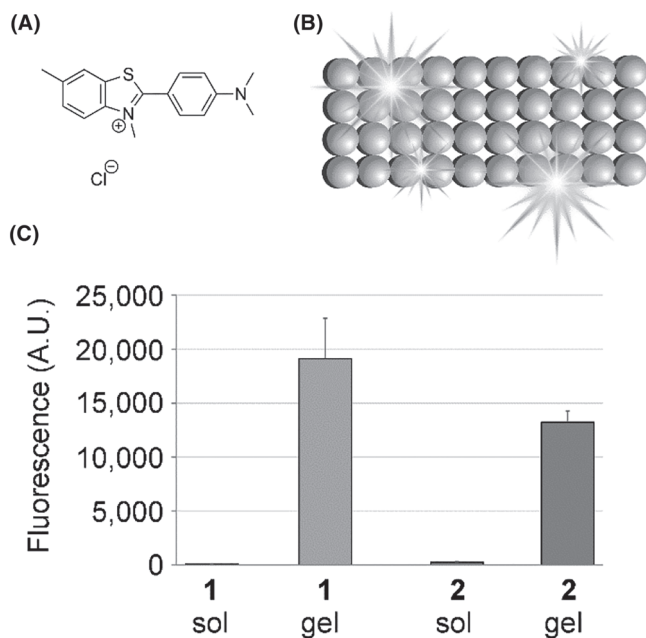


**FIGURE 3** Thioflavin T (ThT) fluorescence assay. (A) ThT chemical structure. (B) schematic showing the assembled tetrapeptide stacks fluorescing upon binding of ThT. (C) ThT fluorescence data for **1** and **2** in the sol (1 mM) and gel (25 mM) states

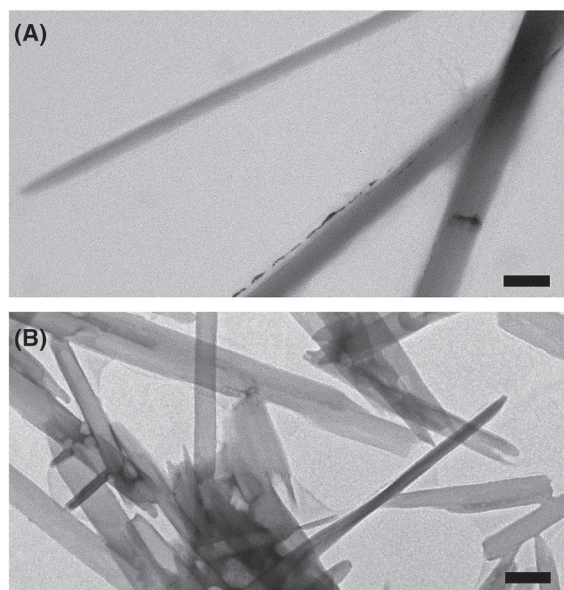


**FIGURE 4** TEM micrographs of (A) **1** and (B) **2** gel samples (25 mM). Scale bar = 500 nm

**TABLE 1** Biocatalytic performance on the hydrolysis of pNPA of **1** and **2**, in the sol (1 mM) or gel (25 mM) states

[pNPA] (mM)	$k_{\text{obs}}$ (1 sol)	$k_{\text{obs}}$ (1 gel)	$k_{\text{obs}}$ (2 sol)	$k_{\text{obs}}$ (2 gel)
0.2	$7.0 \pm 0.7 * 10^{-6} \text{ s}^{-1}$	$5.0 \pm 0.6 * 10^{-5} \text{ s}^{-1}$	$2.4 \pm 0.3 * 10^{-6} \text{ s}^{-1}$	$5.3 \pm 0.6 * 10^{-5} \text{ s}^{-1}$
0.4	$1.8 \pm 0.2 * 10^{-5} \text{ s}^{-1}$	$1.7 \pm 0.3 * 10^{-4} \text{ s}^{-1}$	$3.3 \pm 0.2 * 10^{-5} \text{ s}^{-1}$	$9.3 \pm 0.6 * 10^{-5} \text{ s}^{-1}$
0.6	$2.1 \pm 0.2 * 10^{-5} \text{ s}^{-1}$	<b><math>1.8 \pm 0.2 * 10^{-4} \text{ s}^{-1}</math></b>	$9.8 \pm 0.3 * 10^{-5} \text{ s}^{-1}$	$1.5 \pm 0.3 * 10^{-4} \text{ s}^{-1}$

Note. The highest  $k_{\text{obs}}$  was recorded for **1** (bold). For reference, L-His-D-Phe-D-Phe (25 mM) displayed a  $k_{\text{obs}}$  of  $3.5 * 10^{-4} \text{ s}^{-1}$  with pNPA at 0.2 mM.<sup>17</sup>

Thioflavin T fluorescence was then used as an assay to verify the amyloid character of the assemblies (Figure 3). This dye was reported to bind to amyloid  $\beta$ -sheets composed of at least four consecutive  $\beta$ -strands.<sup>28</sup> The dye association to the hydrophobic groove of the fibril surface limits the rotation between the two aromatic moieties that compose thioflavin T (Figure 3A), leading to fluorescence (Figure 3B).<sup>29</sup> Over the years, it has become the gold standard for the identification of amyloid structures.<sup>30</sup> The assay (Figure 3C) revealed marked fluorescence for both **1** and **2** at high concentration (25 mM), whereas a negligible signal corresponded to the samples in solution (1 mM), suggesting that presence of elongated stacks of amyloid character was significant only at the higher concentration tested. TEM images revealed presence of anisotropic structures both for **1** and **2**, with an average width of  $471 \pm 33 \text{ nm}$  and  $281 \pm 17 \text{ nm}$  ( $n = 100$ ), respectively (Figure 4).

Having established that both compounds self-assembled into amyloid structures that yielded hydrogels at 25 mM, their activity was assessed as biocatalysts for hydrolase mimicry. The well-known 4-nitrophenyl acetate was chosen as a model substrate, because it is easily hydrolysed to the yellow-coloured 4-nitrophenol, which can be easily quantified spectrophotometrically.<sup>31</sup> Product formation was monitored over time, and it was negligible for samples containing the peptides in solution, although the hydrogels displayed mild catalysis (Table 1). There was only a minor difference between **1** and **2**, with **1** generally displaying slightly higher catalytic rates relative to **2**, confirming the literature data that suggested a positive role for a carboxylic moiety adjacent to the His residue.<sup>12</sup> However, a comparison with the catalytic performance of gelling L-His-D-Phe-D-Phe under analogous conditions revealed that presence of Ser negatively affected the catalytic performance, instead of improving it as intended by design.<sup>17</sup> There are many possible reasons to explain this observation. It is possible that Ser could not exert the adjuvant role in catalysis observed in solution,<sup>12</sup> due to steric hindrance in the assemblies. Similarly, the supramolecular structure of these tetrapeptides may be less favourable for biocatalysis, relative to L-His-D-Phe-D-Phe. Furthermore, the assemblies formed by both **1** and **2** at 25 mM were significantly bigger in size relative to the few-nm-wide oligomers and protofibrils observed for L-His-D-Phe-D-Phe at the same concentration,<sup>17</sup> leading to less surface area being available for active participation in catalysis. Other design strategies that may be investigated in the future include the coassembly of different peptide sequences to provide both Ser and His,<sup>32</sup> as well as the introduction of further conformational constraints.<sup>33</sup> Ion-mediated cooperation could also provide attractive alternatives to achieve self-assembly,<sup>34</sup> and improved catalytic performance.<sup>35</sup>

## 4 | CONCLUSION

This work described two heterochiral hydrogelators, that is, D-Ser-D-His-L-Phe-L-Phe and D-Ser-D-His-L-Phe-L-Phe-NH<sub>2</sub> (amidated at the C-terminus), which self-assembled into hydrogels at neutral pH in phosphate buffer. They displayed mild catalytic activity on ester hydrolysis when self-assembled, and the thermoreversibility of their hydrogels suggested a potential use of these, and analogous systems, as *smart* catalysts, whereby activity could be controlled with assembly/disassembly. Unfortunately, presence of Ser did not enhance catalytic activity as intended by design, an indication of the complex relationship that exists between chemical structure of hydrogelator building blocks, and catalytic performance of their supramolecular assemblies. Nevertheless, this study added two further examples of heterochiral short peptides with a (bio)activity residing in their self-organised state and the possibility to reverse assembly with simple physical stimuli warrants scope of further investigations in this research area. Future studies will analyse the effects of other chemical derivatizations in the search of design rules for improved biocatalytic soft matter.

## ACKNOWLEDGEMENTS

The authors would like to acknowledge M. Bisiacchi and P. Bertoncin for their kind technical assistance.

## ORCID

Silvia Marchesan  <https://orcid.org/0000-0001-6089-3873>

## REFERENCES

- Lu Y, Lv Q, Liu B, Liu J. Immobilized Candida antarctica lipase B catalyzed synthesis of biodegradable polymers for biomedical applications. *Biomater Sci*. 2019;7(12):4963-4983.
- Palocci C, Chronopoulou L, Venditti I, et al. Lipolytic enzymes with improved activity and selectivity upon adsorption on polymeric nanoparticles. *Biomacromolecules*. 2007;8(10):3047-3053.
- Paiva KBS, Granjeiro JM. Matrix metalloproteinases in bone resorption, remodeling, and repair. *Prog Mol Biol Transl Sci*. 2017;148:203-303.
- a) Rowley AT, Nagalla RR, Wang SW, Liu WF. Extracellular matrix-based strategies for immunomodulatory biomaterials engineering. *Adv Healthc Mater*. 2019;8:e1801578; b) Su L, Li Y, Liu Y, An Y, Shi L. Recent advances and future prospects on adaptive biomaterials for antimicrobial applications. *Macromol Biosci*. 2019;19:e1900289; c) Szkolar L, Guilbaud J-B, Miller AF, Gough JE, Saiani A. Enzymatically triggered peptide hydrogels for 3D cell encapsulation and culture. *J Pept Sci*. 2014;20(7):578-584.
- Joyce P, Whitby CP, Prestidge CA. Nanostructuring biomaterials with specific activities towards digestive enzymes for controlled

- gastrointestinal absorption of lipophilic bioactive molecules. *Adv Colloid Interface Sci.* 2016;237:52-75.
6. Shang Y, Liu F, Wang Y, Li N, Ding B. Enzyme mimic nanomaterials and their biomedical applications. *ChemBiochem.* 2020;21(17):2408-2418.
  7. Stavrakoudis A, Makropoulou S, Tsikaris V, Sakarellos-Daitsiotis M, Sakarellos C, Demetropoulos IN. Computational screening of branched cyclic peptide motifs as potential enzyme mimetics. *J Pept Sci.* 2003;9(3):145-155.
  8. a) Tomasini C, Castellucci N. Peptides and peptidomimetics that behave as low molecular weight gelators. *Chem Soc Rev.* 2013;42(1):156-172; b) Dehsorkhi A, Castelletto V, Hamley IW. Self-assembling amphiphilic peptides. *J Pept Sci.* 2014;20(7):453-467.
  9. Duncan KL, Ulijn RV. Short peptides in minimalistic biocatalyst design. *Biocatalysis.* 2015;67-81.
  10. a) Zozulia O, Dolan MA, Korendovych IV. Catalytic peptide assemblies. *Chem Soc Rev.* 2018;47(10):3621-3639; b) Singh N, Kumar M, Miravet JF, Ulijn RV, Escuder B. Peptide-based molecular hydrogels as supramolecular protein mimics. *Chem A Eur J.* 2017;23(5):981-993; c) Maeda Y, Makhlynets OV, Matsui H, Korendovych IV. Design of catalytic peptides and proteins through rational and combinatorial approaches. *Annu Rev Biomed Eng.* 2016;18(1):311-328.
  11. Li Y, Zhao Y, Hatfield S, et al. Dipeptide seryl-histidine and related oligopeptides cleave DNA, protein, and a carboxyl ester. *Bioorg Med Chem.* 2000;8(12):2675-2680.
  12. Gorlero M, Wieczorek R, Adamala K, et al. Ser-His catalyses the formation of peptides and PNAs. *FEBS Lett.* 2009;583(1):153-156.
  13. a) Maeda Y, Javid N, Duncan K, et al. Discovery of catalytic phages by biocatalytic self-assembly. *J Am Chem Soc.* 2014;136(45):15893-15896; b) Gulseren G, Khalily MA, Tekinay AB, Guler MO, Mater J. Catalytic supramolecular self-assembled peptide nanostructures for ester hydrolysis. *Chem B.* 2016;4:4605-4611.
  14. Frederix PWJM, Scott GG, Abul-Haija YM, et al. Exploring the sequence space for (tri-)peptide self-assembly to design and discover new hydrogels. *Nat Chem.* 2015;7(1):30-37.
  15. Chan KH, Xue B, Robinson RC, Hauser CAE. Systematic moiety variations of ultrashort peptides produce profound effects on self-assembly, nanostructure formation, hydrogelation, and phase transition. *Sci Rep.* 2017;7(1):12897.
  16. Marchesan S, Vargiu AV, Styan KE. The Phe-Phe motif for peptide self-assembly in nanomedicine. *Molecules.* 2015;20(11):19775-19788.
  17. Garcia AM, Kurbasic M, Kralj S, Melchionna M, Marchesan S. A biocatalytic and thermoreversible hydrogel from a histidine-containing tripeptide. *Chem Commun.* 2017;53(58):8110-8113.
  18. Vargiu AV, Iglesias D, Styan KE, Waddington LJ, Easton CD, Marchesan S. Design of a hydrophobic tripeptide that self-assembles into amphiphilic superstructures forming a hydrogel biomaterial. *Chem Commun.* 2016;52(35):5912-5915.
  19. a) Kralj S, Bellotto O, Parisi E, et al. Heterochirality and halogenation control Phe-Phe hierarchical assembly. *ACS Nano.* 2020;14(12):16951-16961; b) Bellotto O, Kralj S, De Zorzi R, Geremia S, Marchesan S. Supramolecular hydrogels from unprotected dipeptides: a comparative study on stereoisomers and structural isomers. *Soft Matter.* 2020;16(44):10151-10157.
  20. Kapp TG, Rechenmacher F, Neubauer S, et al. A Comprehensive Evaluation of the Activity and Selectivity Profile of Ligands for RGD-binding Integrins. *Sci Rep.* 2017;7(1):39805.
  21. Bobde V, Sasidhar YU, Durani S. Harnessing D-amino acids for peptide motif designs. *Int J Pept Protein Res.* 1994;43:209-218.
  22. Carlomagno T, Cringoli MC, Kralj S, et al. Biocatalysis of D,L-peptide nanofibrillar hydrogel. *Molecules.* 2020;25(13):2995.
  23. Ryan DM, Doran TM, Anderson SB, Nilsson BL. Effect of C-terminal modification on the self-assembly and hydrogelation of fluorinated Fmoc-Phe derivatives. *Langmuir.* 2011;27(7):4029-4039.
  24. Iglesias D, Melle-Franco M, Kurbasic M, et al. Oxidized Nanocarbons-Tripeptide Supramolecular Hydrogels: Shape Matters! *ACS Nano.* 2018;12(6):5530-5538.
  25. Rink H. Solid-phase synthesis of protected peptide fragments using a trialkoxy-diphenyl-methylester resin. *Tetrahedron Lett.* 1987;28(33):3787-3790.
  26. Pignataro MF, Herrera MG, Dodero VI. Evaluation of Peptide/Protein Self-Assembly and Aggregation by Spectroscopic Methods. *Molecules.* 2020;25(20):4854.
  27. Garcia AM, Iglesias D, Parisi E, et al. Chirality Effects on Peptide Self-Assembly Unraveled from Molecules to Materials. *Chem.* 2018;4(8):1862-1876.
  28. Wu C, Biancalana M, Koide S, Shea JE. Binding Modes of Thioflavin-T to the Single-Layer  $\beta$ -Sheet of the Peptide Self-Assembly Mimics. *J Mol Biol.* 2009;394(4):627-633.
  29. Amdursky N, Erez Y, Huppert D. Molecular rotors: what lies behind the high sensitivity of the thioflavin-T fluorescent marker. *Acc Chem Res.* 2012;45(9):1548-1557.
  30. Biancalana M, Koide S. *Biochim. Biophys Acta.* 2010;1804:1405-1412.
  31. Anderson J, Byrne T, Woelfel KJ, Meany JE, Spyridis GT, Pocker Y. The Hydrolysis of p-Nitrophenyl Acetate: A Versatile Reaction To Study Enzyme Kinetics. *J Chem Educ.* 1994;71(8):715.
  32. Zhang C, Xue X, Luo Q, et al. Self-assembled peptide nanofibers designed as biological enzymes for catalyzing ester hydrolysis. *ACS Nano.* 2014;8(11):11715-11723.
  33. a) Kleinsmann AJ, Nachtsheim BJ. A minimalistic hydrolase based on co-assembled cyclic dipeptides. *Org. Biomol. Chem.* 2020;18:102-107; b) Yang X, Wang Y, Qi W, Su R, He Z. Bioorganometallic ferrocene-tripeptide nanoemulsions. *Nanoscale.* 2017;9:15323-15331.
  34. Abul-Haija YM, Scott GG, Sahoo JK, Tuttle T, Ulijn RV. Cooperative, ion-sensitive co-assembly of tripeptide hydrogels. *Chem Commun.* 2017;53(69):9562-9565.
  35. Guler MO, Stupp SI. A self-assembled nanofiber catalyst for ester hydrolysis. *J Am Chem Soc.* 2007;129(40):12082-12083.

## SUPPORTING INFORMATION

Additional supporting information may be found online in the Supporting Information section at the end of this article.

**How to cite this article:** Kurbasic M, Garcia AM, Viada S, Marchesan S. Heterochiral tetrapeptide self-assembly into hydrogel biomaterials for hydrolase mimicry. *J Pep Sci.* 2021; e3304. <https://doi.org/10.1002/psc.3304>